Accepted Manuscript

Step pyrolysis of N-rich industrial biowastes: regulatory mechanism of NO $_x$ precursor formation via exploring decisive reaction pathways

Hao Zhan, Xiuzheng Zhuang, Yanpei Song, Xiuli Yin, Junji Cao, Zhenxing Shen, Chuangzhi Wu

Please cite this article as: H. Zhan, X. Zhuang, Y. Song, X. Yin, J. Cao, Z. Shen, C. Wu, Step pyrolysis of N-rich industrial biowastes: regulatory mechanism of NO $_x$ precursor formation via exploring decisive reaction pathways, *Chemical Engineering Journal* (2018), doi: https://doi.org/10.1016/j.cej.2018.03.099

Step pyrolysis of N-rich industrial biowastes: regulatory mechanism of NO$_x$ precursor formation via exploring decisive reaction pathways

Hao Zhan[a,b,1], Xiuzheng Zhuang[a,b,1], Yanpei Song[a,b], Xiuli Yin[a], Junji Cao[c], Zhenxing Shen[d], Chuangzhi Wu[a] *

a Key Laboratory of Renewable Energy, CAS, Guangdong Provincial Key Laboratory of New and Renewable Energy Research and Development, Guangzhou Institute of Energy Conversion, Chinese Academy of Sciences, Guangzhou 510640, People's Republic of China

b University of Chinese Academy of Sciences, Beijing 100049, People's Republic of China

c Key Lab of Aerosol Chemistry & Physics, Institute of Earth Environment, Chinese Academy of Sciences, Xi'an, 710045, People's Republic of China

d Department of Environmental Sciences and Engineering, Xi'an Jiaotong University, Xi'an, 710049, People's Republic of China

[1] These authors contributed equally to this work.

*Corresponding author at: No. 2, Nengyuan Rd, Wushan Tianhe District, Guangzhou 510640, People's Republic of China. E-mail address: wucz@gzb.ac.cn (C.Z. Wu)

Abstract: Step pyrolysis of N-rich industrial biowastes was used to explore decisive reaction pathways and regulatory mechanisms of NO$_x$ precursor formation. Three typical ones involving medium-density fiberboard waste (MFW), penicillin mycelia waste (PMW) and sewage sludge (SS) were employed to compare the formation characteristics of NO$_x$ precursors during one-step and two-step pyrolysis. Results demonstrated that considerable NH$_3$-N predominated NO$_x$ precursors for one-step pyrolysis at low temperatures, depending on primary pyrolysis of labile amide-N/inorganic-N in fuels. Meanwhile, NO$_x$ precursors differed in the increment of each species yield while resembled in the total yield of 20-45 wt.% among three samples at high temperatures, due to specific prevailing reaction pathways linking with distinctive amide-N types. Subsequently, compared with one-step pyrolysis uniformly (800 °C), by manipulating intensities of reaction pathways at different stages (selecting differential intermediate feedstocks), two-step pyrolysis was capable of minimizing NO$_x$ precursor-N yield by 36-43% with a greater impact on HCN-N (75-85%) than NH$_3$-N (9-37%), demonstrating its great capacity on regulating the formation of NO$_x$ precursors for industrial biowaste pyrolysis. These observations were beneficial to develop effective insights into N-pollution emission control during their thermal reutilization.

1. Introduction

With the sustained industrialization development in China, industrial biowastes have increasingly become an integral origin to biomass resources nowadays. It was reported by Chen et al [1] that the total amount was estimated over 400 million tons per year in 2012. Due to their abundant organic matter and high heating value, thermal-chemical conversion of industrial biowastes, including pyrolysis, gasification and combustion, would be considered as a promising technology to realize their more optimal resource utilization. However, compared to conventional biomass, most of industrial biowastes contained much higher fuel-bound nitrogen (fuel-N) linking with either the intrinsic components (proteins or protein hydrolysates) in themselves or the extrinsic additives (N-compounds) during their utilization processes, such as sewage sludge[2-5], fiberboard[6-8], coffee/tea wastes[6, 8], herb residues[8-10]. Subsequently, fuel-N could be transformed into environmentally harmful gases under thermal-chemical conversion, specifically, NO$_x$ precursors (mainly NH$_3$ and HCN) for pyrolysis and gasification, NO$_x$ for combustion. The emission of these nitrogenous gases would indirectly or directly result in some serious pollutions such as photochemical smog, greenhouse effect, acid rain and stratospheric ozone depletion[11, 12]. Hence, the presence of considerable fuel-N in industrial biowastes has become a critical obstacle to their clean thermal utilization. It is imperative to explore effective technologies for minimizing the emission of harmful nitrogenous gases during thermal utilization of industrial biowastes. Understanding their formation mechanisms is primarily essential and will provide some helpful information.

Generally, pyrolysis lies at the core of all thermal-chemical biomass conversion processes, because it is not only a fundamental approach to the production of high value-added bio-products but also a necessary stage of either gasification or combustion[13]. Thus, detailed information on the evolution pathways of fuel-N to NO$_x$ precursors during their pyrolysis is critical for the optimal control of nitrogenous pollution emission in end-use systems of industrial biowastes. To date, formation mechanisms of NO$_x$ precursors (NH$_3$ and HCN) during industrial biowaste pyrolysis have been widely investigated. Becidan et al.[6] reported that NH$_3$ was more dominant between two species whose yields were greatly affected by both pyrolysis temperature and heating rate (three typical industrial biowastes). Tian et al.[2, 14] found that NH$_3$ and HCN mainly originated from thermal cracking of nitrogen contained in tar (tar-N) and hydrogenation of nitrogen retained in char (char-N) at high temperatures, respectively (sewage sludge and cash trash). Furthermore, besides the consistency in the HCN origin, Cao et al.[4] also indicated that NH$_3$ was main nitrogenous gas whose formation was linked with high protein content in fuel (sewage

2

sludge). Chen et al.[1, 3] confirmed that thermal cracking reaction (for predominant HCN) was associated with nitrile-N and heterocyclic-N in tars, while hydrogenation reaction (for additional NH_3) took place among char-N, HCN and H radical (sewage sludge and mycelia waste). Based on sewage sludge pyrolysis, Wei et al.[5] and Tian et al.[15] established the evolution pathways of char-N and tar-N to NO_x precursors, respectively. Meanwhile, focusing on the pyrolysis of two typical industrial biowastes, Zhu et al.[9] (antibiotic mycelia waste) and Tian et al.[16] (sewage sludge) described the characteristics of nitrogen intermediates in tars and chars (originating from fuel-N) and specified their possible reaction routes in relation to NO_x precursors.

As summarized from the aforementioned studies, the formation of NO_x precursors during pyrolysis of industrial biowastes were basically involved in two aspects: (1) the initial decomposition of fuel-N at primary pyrolysis stage; (2) the further conversion of tar-N and char-N at secondary reaction stage. As for the contributions from two aspects, most studies[1, 2, 6, 14, 16] believed that the conversion of pyrolysis N-intermediates in tars or chars during secondary reactions were chiefly responsible for the NO_x precursors production, especially for the HCN production. In our previous studies[8, 10], the formation characteristic of each NO_x precursor could be clearly characterized by pyrolysis temperature and heating rate. It was further proved that majority of NO_x precursors originated from intense secondary reactions of nitrogen intermediates, which was guaranteed by the simultaneous presence of enough activation energies (high temperatures) and more volatiles/free radicals (rapid pyrolysis). However, a certain amount of NO_x precursors was also produced from primary pyrolysis due to the direct decomposition of some unstable fuel-N (inorganic-N[10], liable amide-N[8]), which was also in accordance with the results of some studies[4, 12, 16].

Hence, it could be indicated that distinctive formation pathways of NO_x precursors were tightly associated with two pyrolysis stages - devolatilisation and secondary reactions. However, due to complex nitrogen functionalities in solid/liquid phases, distinctive formation pathways and various pyrolysis conditions, there was still a lack of coincident quantitative information about the decisive formation route of each NO_x precursor from industrial biowaste pyrolysis. In order to control the emission of NO_x precursors, it is necessary to ascertain the role of each decisive formation route together with its individual contribution to the corresponding NO_x precursor. Based on two different origins of NO_x precursors, feasible investigations on this aspect need to be proposed and explored.

According to the characteristics of pyrolysis system[13, 17], it seems to be difficult for traditional pyrolysis type (one-step pyrolysis) to completely quantify the relationship between NO_x precursors (NH_3 and HCN) and pyrolysis stages. On one hand, low-or medium-temperature pyrolysis was a good way to produce renewable biofuels while it couldn't reflect the effect of tar-N/char-N on NO_x precursors owing to the insufficient secondary reactions. On the

other hand, rapid pyrolysis at high temperatures was an intrinsic part of other thermal-related processes. However, due to the simultaneous occurrence of devolatilisation and secondary reactions, it couldn't distinguish the respective contributions of two aforementioned origins to NO_x precursors. It is currently necessary to find a suitable way to clearly confirm the roles of two origins in the formation of NO_x precursors. Accordingly, step pyrolysis would be a good and promising option, which is defined as follows: (1) primary pyrolysis process (partial or full devolatilisation) of feedstocks at low temperatures to produce intermediate feedstocks; (2) second pyrolysis process of intermediate feedstocks at high temperatures. In such case, it can not only well reflect the effect of initial decomposition of fuel-N from first-step pyrolysis of feedstocks at low temperatures, but also clearly distinguish the contribution of further conversion of tar-N/char-N when comparing the high-temperature pyrolysis of intermediate feedstocks with different nitrogen characteristics. Moreover, this so-called step pyrolysis was directly described by the study of Sharma et al.[18] focusing on the characteristics of tar-N from different step pyrolysis of α–amino acids. Meanwhile, its mechanism and key thought were also indirectly revealed by the studies referring to step gasification (control of tar production in fuel gas)[19] and decoupling combustion (control of NO_x emission in flue gas)[20]. All these suggested that step pyrolysis had its advantage in the separate investigation of different pyrolysis stage and potential in the effective control of nitrogenous pollution emission.

In the present study, three typical industrial biowastes (medium-density fiberboard waste, MFW; penicillin mycelia waste, PMW; and sewage sludge, SS) were employed to reveal decisive reaction pathways of NO_x precursors during their step pyrolysis. Characteristics of NO_x precursors emitted at different temperature ranges during one-step pyrolysis were firstly discussed and compared. On the basis of reaction pathways obtained, two-step pyrolysis was proposed and applied to explore the effects of two origins on the formation of NO_x precursors. Subsequently, the formation of NO_x precursors together with the corresponding evolution of nitrogen in solid phase during two-step pyrolysis were in detail investigated. The objective of this work is to ascertain the roles of primary pyrolysis and secondary reactions in determining the formation of NO_x precursors via two-step pyrolysis, and then to provide guideline on controlling nitrogenous pollution emission from thermal reutilization of industrial biowastes.

2. Material and methods

2.1. Industrial biowaste samples

Three industrial biowastes (MFW, PMW and SS) studied in this work were acquired from a furniture manufacture factory (Yunnan), a medicine production enterprise (Hebei) and a wastewater treatment plant

4

(Guangdong) in China, respectively. Prior to analyses and experiments, feedstock samples were first dried for 24h at 105 °C in an electric oven to remove moisture content, and then ground into 0-300 μm to ensure the same particle size. The proximate and ultimate analyses of samples were conducted in an muffle furnace (MXX1100-30, Shmicrox Co., Ltd., China) and an elemental analyzer (Vario EL cube, Elementaranalyse, Germany), respectively. In addition, calorific value (HHV) of each sample was also determined by an automatic calorimeter (WZR-1T-CII, Changsha Bente Instruments Co., Ltd., China). And the relevant results were listed in Table 1. As seen in Table 1, nitrogen contents in three samples were much higher than those of conventional biomass such as forest and straw residues[11, 21]. MFW was a wood waste from manufacturing process of medium-density fiberboard which was reported to contain around 90% of wood[7]. As a result, it belonged to a lignocellulosic biomass similar to wood[22]. However, PMW and SS were byproducts of antibiotics production and wastewater treatment processes, respectively. Both of them were rich in moisture, protein and saccharide while lack of holocellulose and lignin[23, 24]. Subsequently, these two types could be assigned to nonlignocellulosic biomass. In addition, compared with MFW, two nonlignocellulosic industrial biowastes contained higher ash content, especially for SS. Hence, detailed information on crude fiber content, nitrogen components, biochemical components, ash components and amino acid components were also given in Table S1 (see the Supplementary Materials), which was totally consistent with the above descriptions.

Table 1 Proximate and ultimate analyses of industrial biowaste samples

Samples	Proximate analysis (*wt.*%, db)			HHV (MJ/kg)	Ultimate analysis (*wt.*%, db)				
	VM	FC	Ash		C	H	S	N	O[a]
MFW	78.84	19.50	1.66	18.81	46.84	5.87	0.00	4.11	41.52
PMW	78.51	13.40	8.09	19.28	44.18	6.39	0.53	7.39	33.42
SS	39.56	3.40	57.04	9.41	21.31	3.67	0.48	3.40	14.10

[a] by difference.

2.2. Pyrolysis experiments

Fig.1 A schematic of the experimental setup

A horizontal tubular quartz reactor (44 mm inner diameter and 120 mm length) as shown in Fig. 1 was used to carry out both one-step and two-step pyrolysis experiments. The reactor was heated by a horizontal electric furnace with a temperature controller governing temperature and heating rate. One end of quartz tube was connected with the gas cylinder. High pure argon (99.999%) controlled at 400 mL/min was used to maintain an inert pyrolysis atmosphere. The other end was directly connected with a cold trap in a flexible seal way. The connection segment was set to be a soaking zone to avoid tar condensation. The cold trap containing isopropanol was controlled at 0 °C by ice/water mixture (or ice/brine mixture) to ensure a complete tar absorption. The principal NO_x precursors, NH_3 and HCN, were separately collected by two bubbling absorption lines in parallel due to their high solubility in aqueous solutions[1]. The absorbents for NH_3 and HCN were H_3BO_3 (5 g/L) and NaOH (0.2 mol/L) solutions, respectively. More details of the setup had been described elsewhere[8, 10].

Fig. 2 A flow diagram of experiment procedures

6

Rapid pyrolysis type was employed for all pyrolysis experiments. And a flow diagram of all experiment procedures was schematically shown in Fig. 2. During each one-step pyrolysis, about 3 g of fuel sample was loaded into a ceramic boat and then placed at the cold end of quartz tube. The reactor was then flushed by inert atmosphere and heated up to the desired temperature (300-800 °C with an increment of 100 °C). Subsequently, the ceramic boat was rapidly pushed into the heating zone and held for 30 min to ensure the completion pyrolysis experiment. After this, the ceramic boat was pulled out of the heating zone and cooled down to ambient temperature. The target pyrolysis products were collected and treated as follows: (1) The absorbed NO_x precursors were calculated using the spectrophotometry method; (2) The residual char was weighed and its nitrogen content was determined; (3) The trapped tar was carefully transferred, recovered and weighed, and its nitrogen content was also determined. Each run for one-step pyrolysis was triplicate to take the average value as the final result.

To ascertain the effects of primary pyrolysis and secondary reactions on the formation of NO_x precursors, Two-step pyrolysis was characterized as the first pyrolysis of initial feedstock (raw sample) at low temperatures (300-500 °C with an increment of 100 °C) and the re-pyrolysis of subsequent intermediate feedstock (char derived from the first step) at high temperature (800 °C). Hence, experiment procedure for the first pyrolysis of two-step pyrolysis was completely consistent with one-step pyrolysis. Several runs were repeated at a same low temperature to collect the target char, which was adequately served as the intermediate feedstock for re-pyrolysis. Meanwhile, XPS, proximate and ultimate analyses were also carried out to confirm the properties of intermediate feedstocks. Based on the almost same char yield at a fixed temperature (300, 400 and 500 °C), each primary NO_x precursors were also collected, determined and compared with that in one-step pyrolysis to ensure the reliability. In addition to each run of re-pyrolysis, based on the same experiment method, the intermediate feedstock was pyrolyzed to collect and determine each secondary NO_x precursor. And the weight, nitrogen content and nitrogen functionality referring to secondary residual chars were also determined. Each run for second step of two-step pyrolysis was repeated three times to guarantee reliable results. More detailed information on the procedures could be referred to the previous study[8].

2.3. Analysis methods

Pyrolysis behaviors of three raw industrial biowaste samples were analyzed using a simultaneous thermal analyzer (STA449F3, Netzsch, Germany), which adopted Ar (a flow rate of 40 mL/min) as its atmosphere and followed the heating program as such: heating from 50 °C to 850 °C at a constant heating rate of 15 °C/min.

Nitrogen functionalities in raw samples and chars were analyzed by a X-ray photoelectron spectrometer

(ESCALAB 250Xi, Thermo VG Scientific, UK) equipped with a monochromatic Al Kα X-ray source, which was operating at 150 W with an energy of 1486.68 eV, a spot size of 500 μm in diameter and an electron takeoff angle of 90°. Data acquisition was carried out with a pressure less than 1.E-6 Pa, and in CAE mode with pass energies of 100 and 30 eV for survey and narrow regions, respectively. And all XPS spectra were obtained under identical conditions. For each of them, the N 1s signal was first referenced to the C 1speak at 284.8 eV, and then curve-resolved using peaks with a mixed Gaussian-Lorentzian function of 30%, a FWHM of 1.65 eV and a Shirley type background subtraction. Peaks at 398.8 ± 0.2 eV (pyridinic-N), 399.8 ± 0.3 eV (amide-N), 400.4 ± 0.2 eV (pyrrolic-N), 401.4 ± 0.2 eV (quaternary-N or inorganic-N) and 402-405 eV (oxide-N) were used for the curve resolution. The area of each peak could reflect the relative content of corresponding nitrogen functionality in raw samples and chars. The yield of each nitrogen functionality that was observed in industrial biowaste-derived chars could be calculated as follows[8].

$$Y_{N^*_{char}} = \frac{m_{char} \cdot w_{char-N}}{m_{fuel} \cdot w_{fuel-N}} \cdot \frac{A_{N^*_{char}}}{\sum A_{N^*_{char}}} \tag{1}$$

where $Y_{N^*_{char}}$ was yield of each nitrogen functionality in chars; m_{fuel} and m_{char} were weights of raw industrial biowaste and biowaste-derived char, respectively; w_{fuel-N} and w_{char-N} were nitrogen contents in raw industrial biowaste and biowaste-derived char, respectively; $A_{N^*_{char}}$ was peak area of each nitrogen functionality in XPS spectra.

In each pyrolysis experiment, NO$_x$ precursors (NH$_3$-N and HCN-N) in pyrolysis gas were determined by the combined chemical absorption - spectrophotometry method (HJ 536-2009 and HJ 484-2009). Concentrations of cation NH$_4^+$ and anion CN$^-$ dissolved in each corresponding absorbent were analyzed by a water quality analyzer (DR3900, HACH, USA). The amount of each NO$_x$ precursor could be calculated by gas flow of corresponding absorption line and concentration of corresponding ion, which was expressed in Eqs. (2) and (3).

$$m_{NH3-N} = \frac{14.01 \cdot c_1 \cdot V_1}{\left(18.04 \cdot Q_1 / (Q_1 + Q_2)\right)} \tag{2}$$

$$m_{HCN-N} = \frac{14.01 \cdot c_2 \cdot V_2}{\left(26.02 \cdot Q_2 / (Q_1 + Q_2)\right)} \tag{3}$$

where m_{NH3-N} and m_{HCN-N} were amounts of NH$_3$-N and HCN-N in pyrolysis gas, respectively; c_1 and c_2 were concentrations of NH$_4^+$ and CN$^-$ in solutions, respectively; V_1 and V_2 were volumes of corresponding absorbents, respectively; Q_1 and Q_2 were gas flows of absorption lines for NH$_3$ and HCN, respectively.

In addition, yield of each NO$_x$ precursor during one-step and two-step pyrolysis could be determined by Eqs. (4) and Eqs. (5), respectively.

8

$$Y_{one} = {m_{one}} \Big/ {\left(m_{Fs1} \cdot w_{Fs1-N} \right)} \qquad (4)$$

$$Y_{two} = {m_{two-1}} \Big/ {\left(m_{Fs1} \cdot w_{Fs1-N} \right)} + {m_{two-2}} \Big/ {\left(m_{Fs2} \cdot w_{Fs2-N} \right)} \cdot Y_{char-N} \qquad (5)$$

where Y_{one} and Y_{two} were total yield of NO_x precursor-N (NH_3-N or HCN-N) during one-step and two-step pyrolysis, respectively; m_{one} was amount of NO_x precursor-N (NH_3-N or HCN-N) in pyrolysis gas during one-step pyrolysis; m_{two-1} and m_{two-2} were amounts of NO_x precursor-N (NH_3-N or HCN-N) in pyrolysis gas for first and second step during two-step pyrolysis, respectively; m_{Fs1} and w_{Fs1-N} were weight and nitrogen content of initial feedstock (raw sample), respectively; m_{Fs2} and w_{Fs2-N} were weight and nitrogen content of intermediate feedstock (char derived at T), respectively; Y_{char-N} was yield of char-N from fuel-N at a certain temperature (T) after first step during two-step pyrolysis.

3. Results and discussion

3.1. Pyrolysis behaviors of industrial biowastes

Prior to the discussion, thermogravimetric analysis was used to identify pyrolysis behaviors of industrial biowastes. Subsequently, weight loss (TG) curves and corresponding derivative thermogravimetric (DTG) curves of three types were presented in Fig. 3.
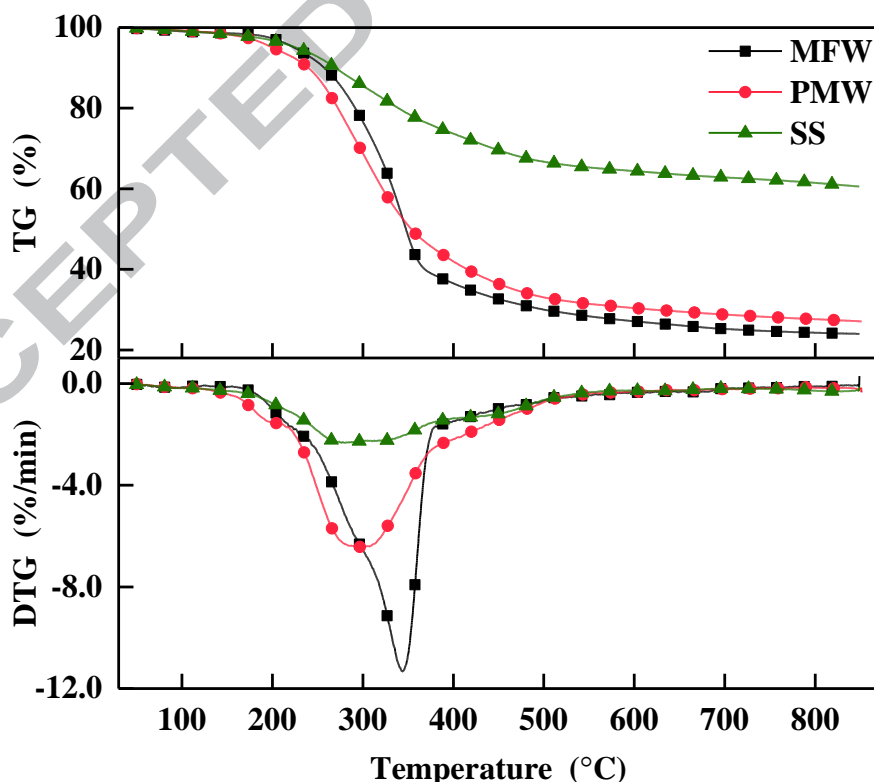

Fig. 3 TG and DTG curves of industrial biowastes at 15 °C·min⁻¹ under Ar atmosphere

As shown in Fig. 3, predominant weight loss was observed at a similar temperature range of 150-500 °C for each

9

biowaste during thermal degradation process, which was almost consistent with the complete devolatilisation stage during biomass pyrolysis[13, 25]. Nevertheless, pyrolysis behaviors of industrial biowastes had great differences in both overall weight loss and DTG peaks. On one hand, the overall weight loss in TG curves were observed with a sequence of MFW (~75.7 wt%) > PMW (~72.4 wt%) > SS (~38.6 wt%) due to the diversities in their volatile matter and ash contents. On the other hand, MFW had a sharp main DTG peak at around 344 °C with a strong maximum reaction rate of 11.3 %·min^{-1}. By comparison, the main DTG peaks for PMW and SS were similarly showing a wide temperature range of 275-315 °C and 260-330 °C, with the corresponding reaction rate of 6.3 %·min^{-1} and 2.3 %·min^{-1}, respectively.

To be more specific, it was clearly illustrated that MFW presented a more dramatic thermal decomposition at a higher pyrolytic temperature compared with other two industrial biowastes, which could be well explained by two aspects: (1) With regard to the intensity of DTG peak (MFW > PMW > SS), it largely depended on the content of organic matters in them (see Table 1); (2) As for the occurrence of DTG peak, the higher temperature for MFW could be attributed to the initial degradation of stable proteins and holocelluloses[25] due to its woody characteristic[7]. While, the lower wide temperature range for PMW and SS might be ascribed to the decomposition of special organic matters (proteins, amino acids, saccharides and other carbohydrates) originating from their specific production processes[1, 4, 26]. Most importantly, it should be noted for three samples that each DTG curve had an obvious shoulder peak at a much lower temperature. The secondary shoulder peak nearby 265 °C for MFW have indicated the decomposition of polyamide structure in it[7]. Meanwhile, the shoulder peaks at 195-215 °C for PMW and at 175-215 °C for SS have revealed that the inorganic-N structures in them started to decompose at a quite low temperature[10, 16]. It was clearly indicated from pyrolysis behaviors of industrial biowastes that the relevant nitrogen functionalities in fuels had a sequential thermal stability to the temperature, which would play an important role in the formation of NO$_x$ precursors during pyrolysis of industrial biowastes.

3.2. Formation characteristics of NO$_x$ precursors during one-step pyrolysis

3.2.1. NO$_x$ precursors derived at low temperatures

It was reported that the formation of NO$_x$ precursors at low temperatures was largely linked with the initial thermal degradation of fuel-N during biomass/biowaste pyrolysis[3, 8, 14, 16]. The main pyrolysis reactions at this stage involved the release of volatile matter and the formation of char. According to the main weight loss caused by devolatilisation reaction (see TG/DTG curves in Fig. 3), 300-500 °C was selected as the low temperature range. Hence, characteristics of NO$_x$ precursors derived from low-temperature pyrolysis of three samples were displayed

in Fig.4. Meanwhile, the corresponding nitrogen functionalities in raw samples were also attached.
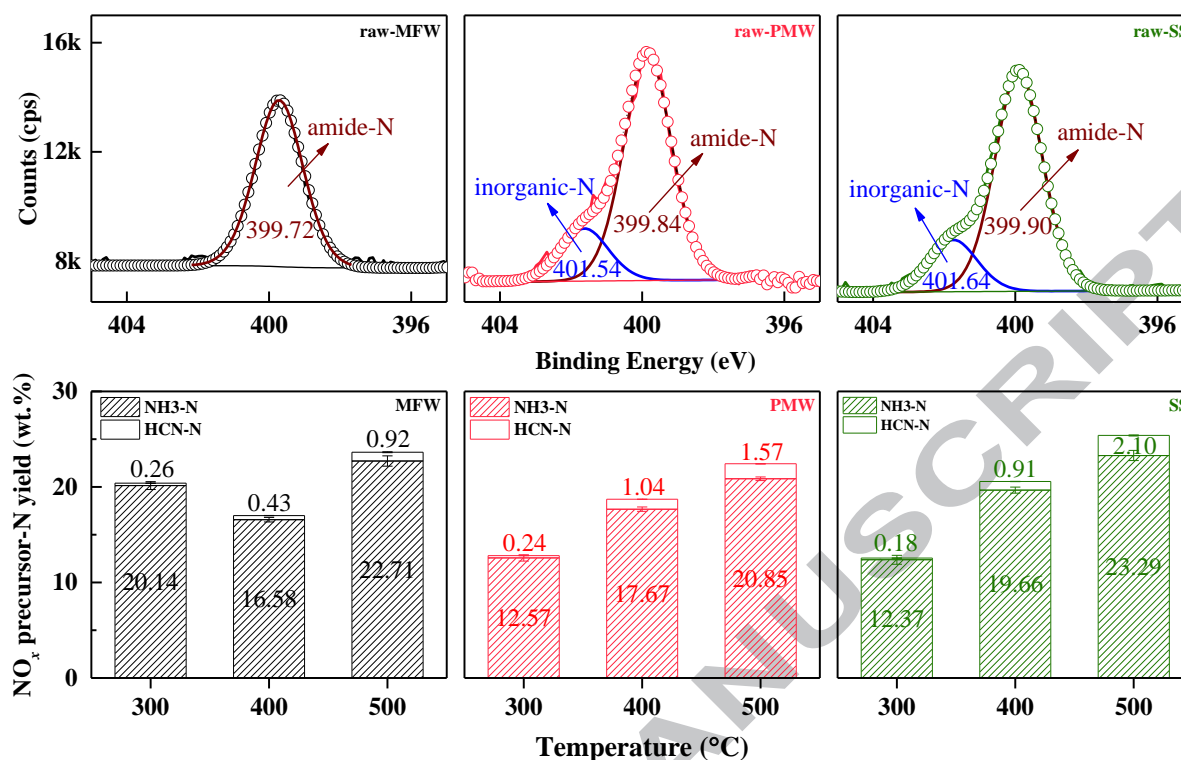

Fig. 4 Characteristics of fuel-N and each NO_x precursor (NH_3-N and HCN-N) derived at low temperatures

XPS nitrogen (1s) spectra of three samples revealed that amide-N types (399.8 ± 0.3 eV) were the overwhelming nitrogen functionalities in fuels. Besides this, another XPS peak at 401.4 ± 0.2 eV with the area ratio of approximate 19.0 % was also observed for both PMW and SS, which could be identified as inorganic-N type based on the sounder results in earlier studies[10, 27]. In addition, there would be some difference on the binding energy of amide-N for each sample. The distinctive one (399.72 eV) for MFW could further demonstrate that its predominant amide-N was in the form of polyamide instead of protein[7]. On the contrary, the more similar ones (399.84 and 399.90 eV) for PMW and SS was caused by the overwhelming presence of protein/amino acid structures in two nonlignocellulosic biowastes[23, 24]. Subsequently, it was interesting to note that information on nitrogen functionalities in fuels were well consistent with the above results of DTG analysis in Fig. 3 and nitrogen/amino acid component analyses in Table S1 (see the Supplementary Materials). When it came to low-temperature pyrolysis of amide-N/inorganic-N systems, the possible reaction pathways of fuel-N to NO_x precursors could be summarized in Fig. 5 according to some previous studies[5, 8, 15, 16, 28, 29].
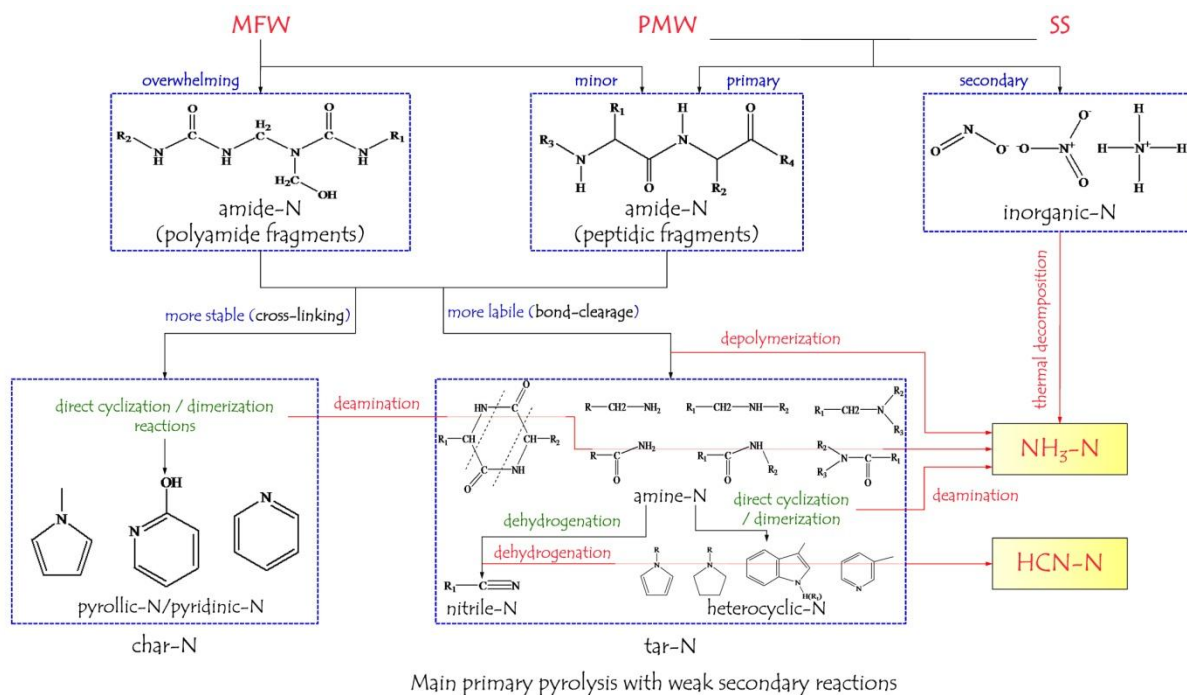
Fig. 5 Possible reaction pathways of fuel-N to NO_x precursors for low-temperature pyrolysis of

amide-N/inorganic-N systems

It was suggested that more labile and stable amide-N types tended to be evolved into new N-intermediates in tars (amine-N and heterocyclic-N) and heterocyclic-N (pyridinic-N and pyrrolic-N) in chars by bond-clearage and cross-linking reactions during devolatilisation stage, respectively. Simultaneously, the deamination and dehydrogenation reactions occurring at this stage were chiefly responsible for the production of NH_3 and HCN, respectively. As seen in Fig. 4, NH_3-N was increasingly produced at a considerable yield to the temperature, which was mainly ascribed to prevailing deamination reactions caused by the presence of more labile amide-N types in three samples. Specifically, for MFW, an obvious drop on NH_3-N yield from 300 to 400 °C was ascribed to the maximum release of NH_3 at around 300 °C as well as the overwhelming emission of HNCO (contributing to NH_3 in wet sampling system) at 250-400 °C during polyamide pyrolysis[7]; for PMW and SS, the direct decomposition of inorganic-N could also make some contribution on NH_3-N yield[16]. HCN-N yield was observed at an ignorable level, suggesting that the sustained dehydrogenation reaction was difficult to take place at low temperatures. This observation was also consistent with the result in our previous study[8]. It was clearly concluded that a remarkable amount of NH_3 overwhelmingly dominated NO_x precursor species derived from low-temperature pyrolysis (mainly referring to devolatilisation stage) of three samples, which was strongly linked with deamination reactions of liable amide-N types in fuels or their subsequent N-intermediates.

3.2.2. NO_x precursors derived at high temperatures

When pyrolyzing at high temperatures, primary pyrolysis (devolatilisation and char formation) and secondary reactions (thermal cracking of tar and char) had occurred simultaneously[30]. Subsequently, the formation of NO_x precursors depended on not only primary pyrolysis of fuel-N but also secondary cracking of char-N/tar-N. Fig. 6 illustrated the change on each NO_x precursor-N (NH_3-N and HCN-N) yield derived from high-temperature (600-800 °C) pyrolysis of three samples.
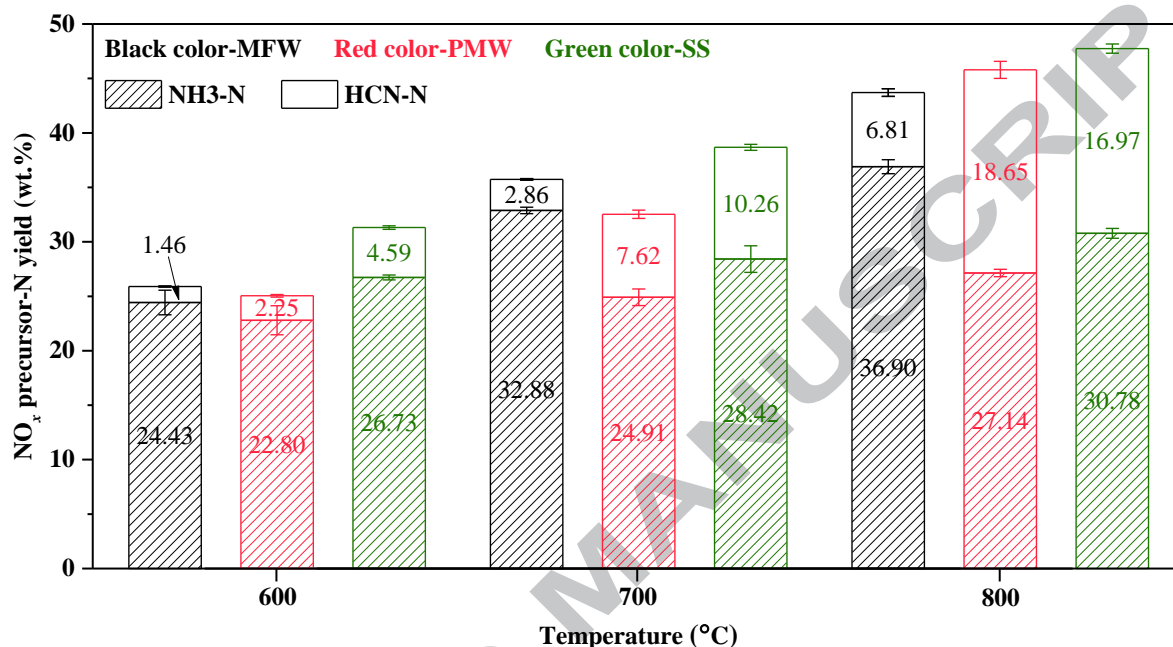

Fig. 6 Characteristics of NO_x precursors-N (NH_3-N and HCN-N) derived from one-step pyrolysis at high temperatures

When temperature went up during high-temperature range, both NH_3-N and HCN-N yields had an obvious increase for each industrial biowaste, which was attributed to the fact that higher temperature could provide more activation energies in favor of the formation of NO_x precursors[31]. Comparing two NO_x precursor species, it was uniformly observed for three samples that NH_3-N was still produced more dominantly than HCN-N at high temperatures. The possible reaction pathways of fuel-N to NO_x precursors based on high-temperature pyrolysis of amide-N/inorganic-N systems were in detail illustrated (see Fig. 7).
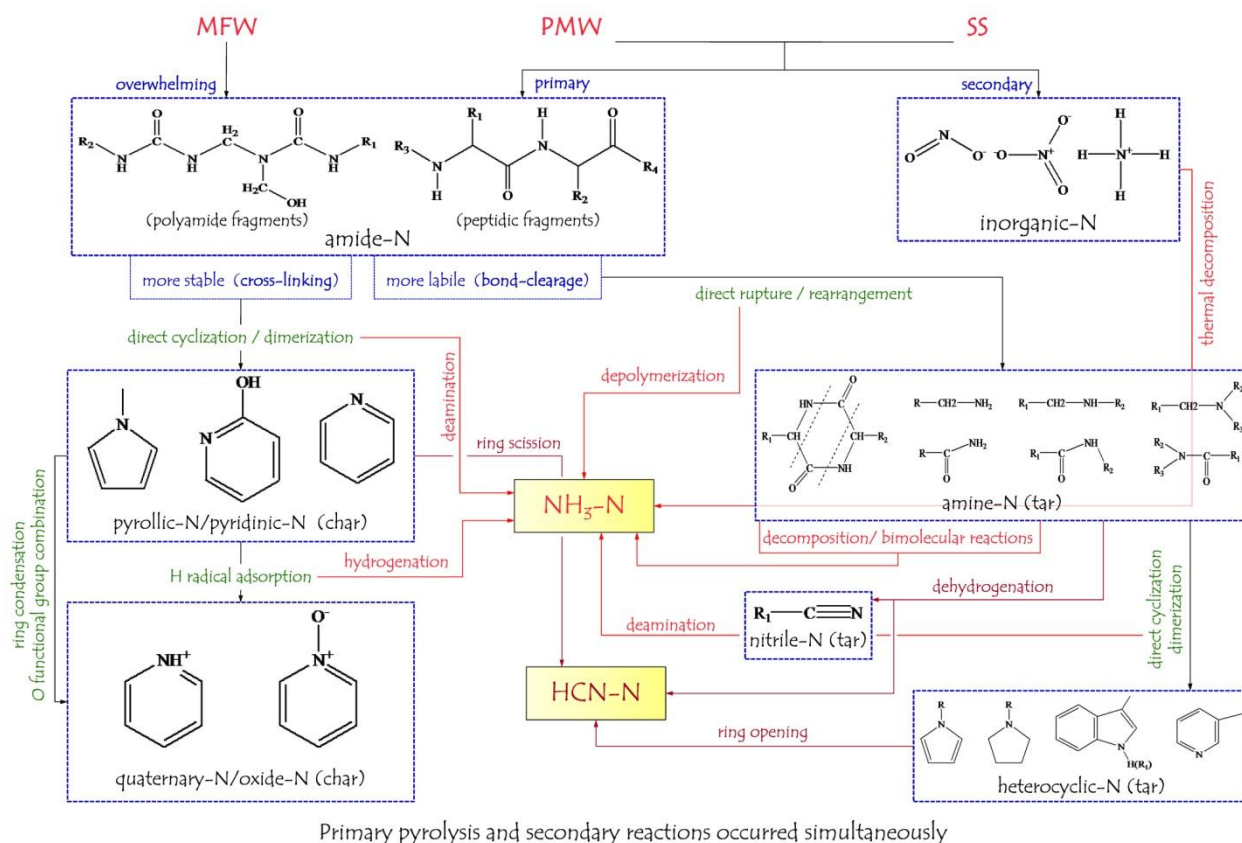
Fig. 7 Possible reaction pathways of fuel-N to NO$_x$ precursors for high-temperature pyrolysis of

amide-N/inorganic-N systems

For one thing, the contributions on NH$_3$-N yield at high temperatures could be ascribed to three aspects: (1) the depolymerization of labile amide-N and decomposition of inorganic-N (fuel-N)[3, 15, 29]; (2) the deamination, decomposition and bimolecular reactions of amine-N (tar-N)[21, 28]; (3) the hydrogenation of heterocyclic-N (char-N) with the help of H radical[8, 12, 16]. For another, the production of HCN-N at high temperatures depended on the sustained dehydrogenation of linear amides (fuel-N or tar-N)[8, 32], the dehydrogenation of imines from thermal cracking of cyclic amide intermediates (tar-N)[21, 30], and the ring-opening of heterocyclic-N (char-N and tar-N)[5, 8, 16]. Consequently, the predominance of NH$_3$-N demonstrated that the additive effect of NH$_3$ formation pathways (deamination, decomposition and hydrogenation reactions) was much stronger than that of HCN formation pathways (dehydrogenation and ring-opening reactions) at high temperatures. Moreover, the increment of each NO$_x$ precursor yield was observed with a sequence of NH$_3$-N (12.47 wt.%) > HCN-N (5.35 wt.%) for MFW while HCN-N (12.38-16.40 wt.%) > NH$_3$-N (4.05-4.34 wt.%) for both PMW and SS when temperature increased from 600 to 800 °C. This finding might be explained by that the prevailing formation pathway of each NO$_x$ precursor was different among three samples due to their distinctive nitrogen functionalities in fuels (polyamide structure in MFW, protein/amino acid/ inorganic-N structures in PMW and SS).

14

3.2.3. Nitrogen distribution in relation to NO$_x$ precursors during one-step pyrolysis

To further elucidate the characteristics of NO$_x$ precursors emitted at different temperature ranges, nitrogen distribution in NO$_x$ precursors, chars and tars derived from one-step pyrolysis of three samples were compared, as depicted in Fig. 8.
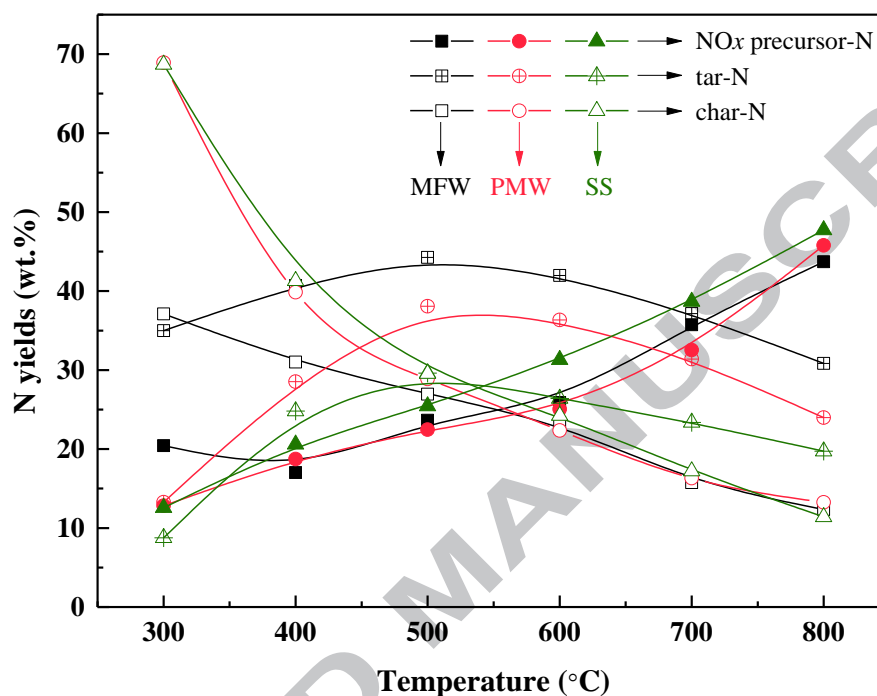

Fig. 8 Nitrogen distribution in different phases during one-step pyrolysis

It was observed that char-N yield had a continuous decrease when temperature was increasing, which might be attributed to that the decomposition of amide-N and inorganic-N types at higher temperatures would cause nitrogen to be cracked into volatility and released out[16]. Particularly, char-N yield of PMW showed a similar tread with that of SS, but either of them was much higher than that of MFW at low temperatures (300-500 °C), perhaps due to the motivation in nitrogen release from more labile amide-N (polyamide) in MFW[7] and the inhibition in nitrogen evolution from higher ash content in PMW and SS[27]. Regarding to tar-N yield of each sample, it went up first with temperature increasing from 300 to 500 °C, as more nitrogen evolved as large molecule volatility; but it would be cracked into light gas phase with temperature increasing further, leading to the drop on tar-N yield. The change on tar-N yield could also indicate that the secondary reactions were getting more obvious above 500 °C. Meanwhile, tar-N yield of three samples was observed with the sequence of MFW > PMW > SS at all temperature range, which was not only dependant on its sequential formation intensity at devolatilisation stage (the aforementioned explanation on change of char-N yield at low temperatures), but also linked with its similar consumption intensity at main secondary reaction stage (a close decrement of tar-N yield for each sample). However, NO$_x$ precursor-N

15

yield showed a mild difference among three samples, keeping a constant increase with the increasing temperature. At low temperatures, NH_3-N mainly predominated NO_x precursor-N, consequently, the sequential thermal stability of fuel-N (inorganic-N < polyamide < protein/amino acid) resulted in the difference on NO_x precursor-N yield for three samples. At high temperatures, although NO_x precursor-N (NH_3-N and HCN-N) of each biowaste differed in their prevailing formation pathways, the total yield was varying at a range of 20-45 wt.% from 500 to 800 °C, having little relationship with biowaste types. This finding was well in accordance with our previous studies[10, 31], and also corresponded to other previous results[3, 4, 6]. Nevertheless, as for the contribution to the formation of NO_x precursors at high temperatures, the partitioning between primary pyrolysis stage and secondary reaction stage (referring to the effects of char-N and tar-N) could be clearly reflected, which was further ascertained in the following discussion.

3.3. Formation characteristics of NO_x precursors during two-step pyrolysis

3.3.1. Properties of intermediate feedstocks

It was revealed in Fig. 3 that the devolatilisation of three samples could be almost completed when temperature reached up to 500 °C. Hence, it was appropriate to select char products produced from one-step pyrolysis at low temperatures (300-500 °C) as the intermediate feedstocks, which was well able to reflect the characteristics of both partial and full devolatilisations. Regarding to nitrogen functionalities in these intermediate feedstocks, their N 1s XPS spectra were mainly deconvoluted into four peaks: amide-N, pyridinic-N, pyrrolic-N and quaternary-N, as displayed in Fig. S1 (see the Supplementary Materials). By integrating their peak areas in each N 1s XPS spectra, the relative content of these nitrogen functionalities in intermediate feedstocks were listed in Table 2. In addition, the relevant proximate and ultimate analyses were also involved.

Table 2 Properties of intermediate feedstocks

Intermediate feedstocks	Proximate and ultimate analyses (*wt*.%, db)								Ratio of nitrogen functionalities (%, db)			
	VM	FC	Ash	C	H	S	O^a	N	N-A[b]	N-6[c]	N-5[d]	N-Q[e]
MFW-300	65.86	31.82	2.32	56.29	5.53	0.00	33.57	2.29	47.91	27.16	24.93	-
MFW-400	32.02	63.50	4.48	70.47	4.23	0.00	17.33	3.49	-	37.11	62.89	-
MFW-500	22.45	71.96	5.59	75.75	3.43	0.00	11.46	3.77	-	43.16	45.68	11.16
PMW-300	59.79	26.75	13.46	54.35	5.20	0.40	17.93	8.66	48.40	25.51	26.09	-
PMW-400	32.49	46.23	21.28	55.92	3.89	0.41	10.42	8.08	10.06	40.27	49.67	-
PMW-500	20.07	53.16	26.77	54.89	2.69	0.43	7.79	7.43	-	46.70	47.28	6.02

SS-300	26.64	5.06	68.30	18.21	2.49	0.36	7.81	2.83	52.67	16.25	22.71	8.37[f]
SS-400	16.00	5.95	78.05	13.47	1.79	0.33	4.42	1.94	16.90	32.30	41.12	9.68
SS-500	9.85	5.92	84.23	11.12	1.31	0.34	1.49	1.51	-	39.15	43.55	17.30

[a] by difference, [b] N-A:amide-N, [c] N-6: pyridinic-N, [d] N-5: pyrrolic-N, [e] N-Q: quaternary-N, [f] the coexistence of quaternary-N and inorganic-N.

It could be seen from Table 2 that pyridinic-N and pyrrolic-N were two nitrogen functionalities with a varying ratio in each intermediate feedstock produced at different devolatilisation temperature. When comparing them along with devolatilasation process (from 300 to 500 °C), relative contents of both pyridinic-N and pyrrolic-N increased significantly, originating from the direct cyclization of some amino acids with a long enough chain[33, 34] or the dimerization of some aliphatic amino acids[35] through deamination, dehydration, decarboxylation or dehydrogenation reactions (see Fig. 5). As a consequence, amide-N behaved a swift decreasing ratio, even reaching to a vanishing value (e.g. intermediate feedstock-500). Meanwhile, quaternary-N was formed with an increasing ratio, which mainly resulted from the conversion of pyridinic-N through ring condensation and H radical adsorption reactions[8, 36] (see Fig. 7). And it was also observed that the occurrence of quaternary-N was more obvious for intermediate feedstocks of SS. It needed to point out that the relative content of quaternary-N in SS-300 had an abnormal value (8.37%) closer to that in SS-400, which might be explained by the coexistence of quaternary-N and inorganic-N (the initial formation of quaternary-N took place earlier than the complete decomposition of inorganic-N in SS) due to their same binding energy positions[16, 21, 27]. In addition, both hydrogen and oxygen contents in intermediate feedstock were lower than that in raw feedstock and declining with the devolatilasation process for each biowaste, which was one of important factors affecting the formation of NO_x precursors at secondary reaction stage. However, nitrogen content in intermediate feedstock showed different changes among biowaste types. For one thing, both MFW and SS had a lower value while PMW behaved a higher one compared with raw feedstock, reflecting that fuel-N in PMW (amide-N) was more difficult to release than that in other two samples; for another, nitrogen content showed a decreasing tread for both PMW and SS while presented an increasing tendency for MFW along with devolatilasation process (from 300 to 500 °C), perhaps caused by the different abundant release stages of specific amide-N types (polyamide, protein/amino acid) (see TG/DTG curves in Fig. 3).

3.3.2 NO_x precursors derived from re-pyrolysis of intermediate feedstocks

By mean of re-pyrolyzing these intermediate feedstocks at 800 °C, each NO_x precursor-N yield derived from this

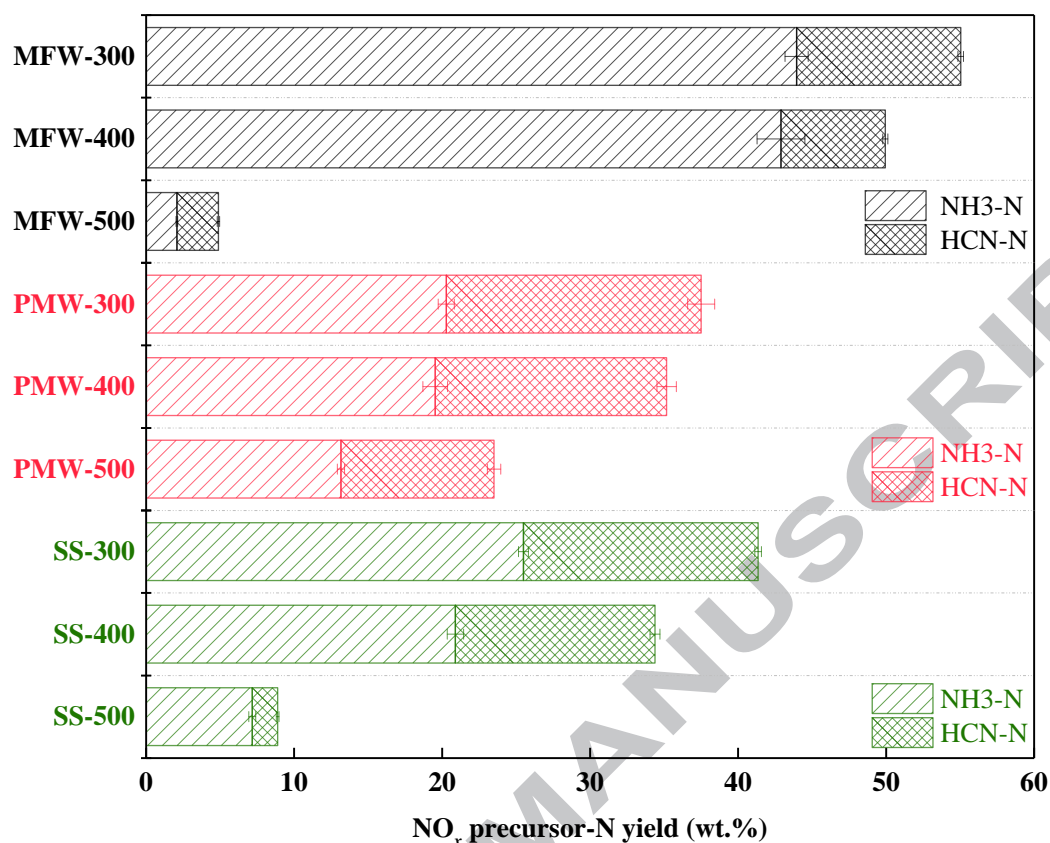process for three samples was obtained, and the results were illustrated in Fig. 9.

Fig. 9 Characteristics of NO_x precursors derived from the re-pyrolysis (800 °C) of intermediate feedstocks

A similar tread for three industrial biowastes was clearly noticed during re-pyrolysis process: when the target intermediate feedstocks were sequentially switching from 300 to 500 °C, the production of both NH_3-N and HCN-N would be shrinking in varying degrees, remarkably leading a gradual drop on their total yield. A specific expressions and explanations were stated here.

(1) Regarding to MFW, NO_x precursor-N yield for MFW-300 and MFW-400 maintained a considerable value which was even higher than that for raw feedstock. As seen in Table 2, MFW-300 contained main amide-N together with a portion of pyrrolic-N/pyridinic-N while MFW-400 was mainly in form of pyrrolic-N and pyridinic-N. Of course, hydrogen and oxygen elements were still sufficiently retained. Subsequently, according to the origins of NO_x precursors[5, 8, 16, 21, 32], hydrogenation and ring scission reactions of pyrrolic-N/pyridinic-N resulted in NH_3 and HCN for re-pyrolysis of MFW-400, respectively; while, besides the aforementioned routes, both deamination/decomposition/bimolecular reactions (for NH_3) and dehydrogenation reaction (for HCN) could also contribute to NO_x precursors for re-pyrolysis of MFW-300 due to the presence of amide-N. It could be concluded that the hydrogenation of heterocyclic-N was more intense than other formation pathways in polyamide system, leading an equal NH_3-N yield. However, MFW-300 had a higher HCN-N yield than MFW-400, perhaps attributed

to its extra contribution of amide-N. When re-pyrolyzing MFW-500 at 800 °C, NO_x precursor-N yield decreased to a quite low value, which could be explained that a limited level of H radical provided and a certain amount of more stable heterocyclic-N (quaternary-N) formed largely hindered the relevant secondary reactions.

(2) As for PMW and SS, intermediate feedstocks at 300 and 400 °C had a similar remarkable NO_x precursor-N yield (the similar characteristic as MFW), but the total yield was lower than that for both the respective raw feedstock and the corresponding MFW intermediate feedstock. Subsequently, on one hand, compared to protein/amino acid system, it was inferred (from distinctions) that nitrogen intermediates from polyamide system could exhibit stronger secondary reactions (producing NO_x precursors) base on their diversity on the structure and thermal degradation characteristics[6, 8]. One the other hand, it was also reflected (from similarities) that relevant reaction pathways of pyrrolic-N/pyridinic-N at secondary reaction stage were getting more prevailing from intermediate feedstock-300 to intermediate feedstock-400. As a result, NO_x precursor-N yield would be enhanced, basically recouping their loss caused by the decrease of amide-N. When referring to intermediate feedstock-500, NO_x precursor-N yield had an obvious decline for both PMW and SS, which was also due to the weaker secondary reactions caused by a similar property situation as MFW-500. However, PMW-500 still kept a relative higher value, maybe related to its more unstable heterocyclic-N and nitrogen content compared to SS-500.

Therefore, based on re-pyrolysis of intermediate feedstocks, it was obtained that the stability of heterocyclic-N and the sufficiency of H radical were two essential factors determining NO_x precursor-N yield at secondary reaction stage. To further demonstrate the aforementioned conclusions, characteristics of nitrogen functionalities in ultimate chars (800 °C) from different step-pyrolysis were compared in Fig. 10.
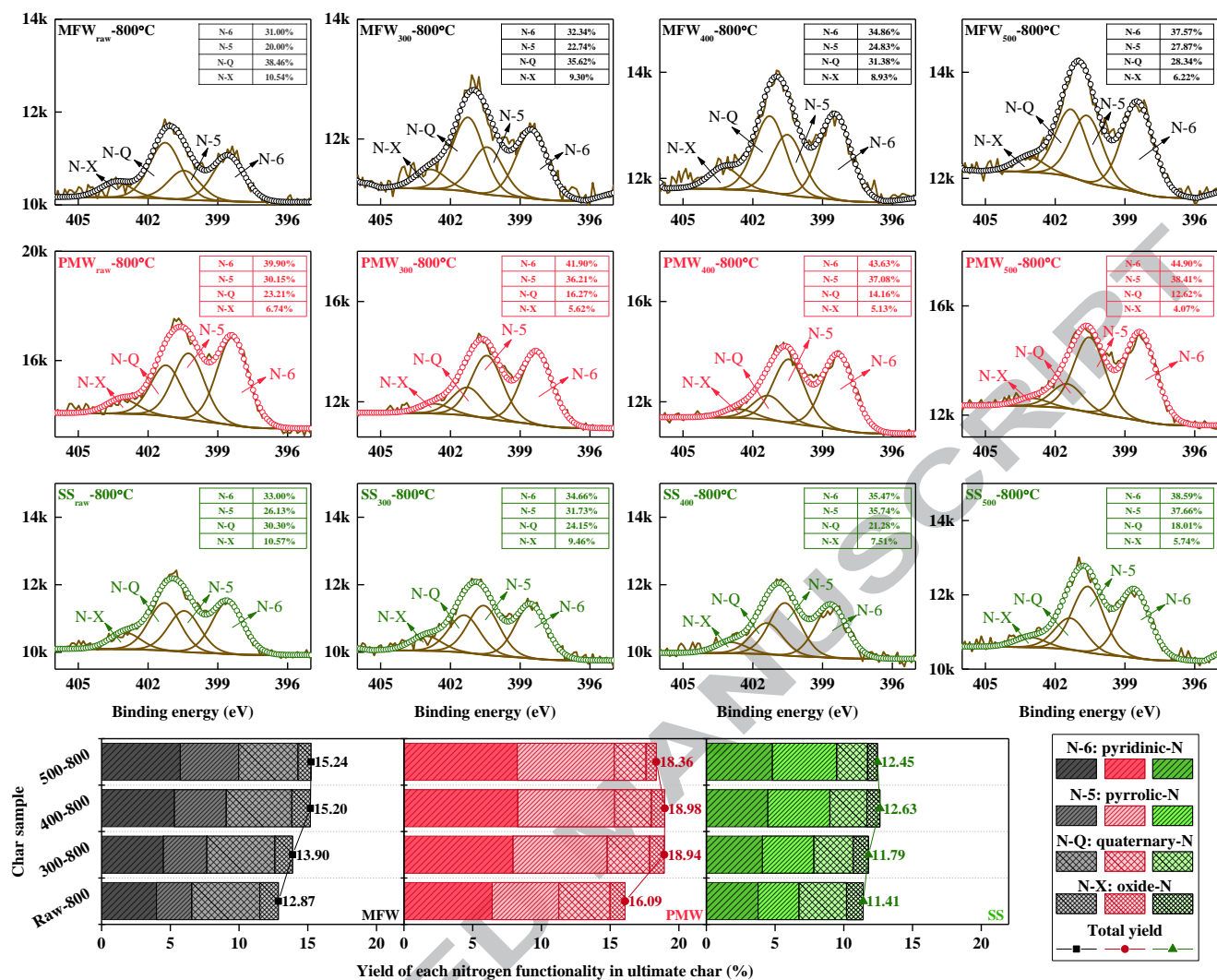
19

Fig. 10 Characteristics of nitrogen functionalities in ultimate chars from different step-pyrolysis

As shown in Fig.10, four nitrogen functionalities were uniformly observed in the N 1s XPS spectra of ultimate chars, including pyrrolic-N, pyridinic-N, quaternary-N and oxide-N. Based on the nitrogen functionalities in (raw or intermediate) feedstocks, nitrogen evolution in solid phase during their high-temperature pyrolysis could be summarized in two aspects (a detailed description in Fig. 7): (1) pyrrolic-N and pyridinic-N resulted from the cyclization and rearrangement of more stable amide-N via crossing-linking reactions[12, 21]; (2) both of them would be simultaneously converted into larger more stable quaternary-N (ring condensation or H radical adsorption reactions) and oxide-N (O functional group combination reaction)[5, 8]. Meanwhile, some of them containing active N-sites would be easily ring-cracked (into HCN) or hydrogenated (into NH_3)[15, 37], accountable for the main formation of NO_x precursors at secondary reaction stage. Subsequently, change on their relative contents in each ultimate char from different step-pyrolysis could also reflect the intensity of secondary reactions.

When sequentially comparing ultimate chars produced from raw feedstock to intermediate feedstock-500, it was observed for three samples that relative peak areas of pyrrolic-N and pyridinic-N were increasing while that for

other two nitrogen functionalities were decreasing. Furthermore, combining the peak area ratio with char-N yield, each nitrogen functionality yield in ultimate chars from different step-pyrolysis was also depicted. It was seen that total yield of pyrrolic-N and pyridinic-N presented a gradual increment with the changing ultimate chars from raw to intermediate feedstocks. On the contrary, total yield of quaternary-N and oxide-N showed a constant decrement under the same condition. As a result, compared to the pyrolysis of raw feedstock, it was demonstrated that the conversion of heterocyclic-N (pyrrolic-N/pyridinic-N) to more stable ones (quaternary-N/oxide-N) would be inhibited (referring to weaker secondary reactions) for re-pyrolysis of intermediate ones. Besides, this inhibition became more obvious for the intermediate feedstock at a higher devolatilasation temperature. Furthermore, this inhibiting effect would inevitably hinder the formation of NO_x precursors at secondary reaction stage, corresponding to the gradual drop on NO_x precursor-N yield for re-pyrolysis of intermediate feedstocks, especially for intermediate feedstock-500.

3.3.3. NO_x precursors derived from two-step pyrolysis

Based on the aforementioned discussion, each NO_x precursor-N (NH_3-N and HCN-N) yield produced at 800 °C via different two-step pyrolysis of three samples were calculated using Eqs. (5), and compared with the corresponding results of one-step pyrolysis, as illustrated in Fig 11.
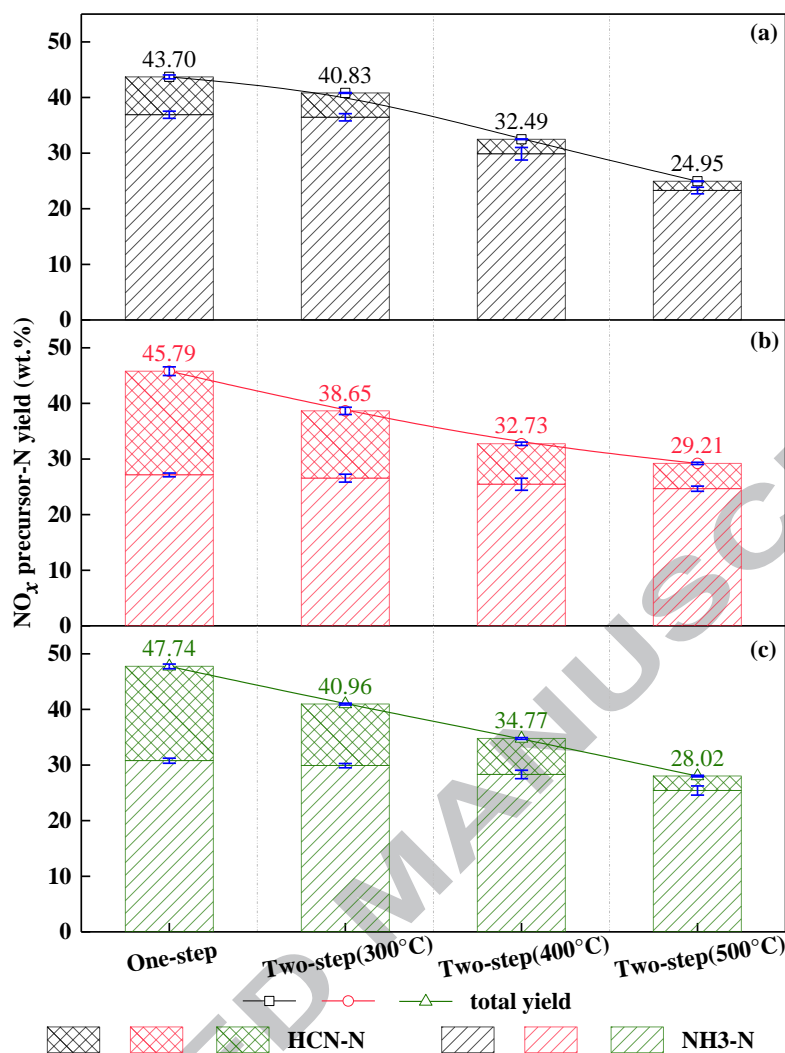
21

Fig. 11 Comparisons of each NO_x precursor-N (NH_3-N and HCN-N) yield derived from one-step and two-step pyrolysis: (a)-MFW; (b)-PMW; (c)-SS

It was noted that total yield of NO_x precursor-N for two-step pyrolysis was all obviously lower than that for one-step pyrolysis. Meanwhile, it behaved a constant decrease for specific two-step pyrolysis when the selection of intermediate feedstock was sequentially ranging from 300 to 500 °C. Specifically, when comparing these step pyrolysis types sequentially from one-step to two-step (300°C, 400°C and 500°C) for PMW, SS and MFW, NH_3-N yield exhibited different degrees of decrease with maximal values of 2.48, 5.37 and 13.62 wt.% (by 9, 17 and 37%); HCN-N yield suffered dramatic decrements with maximal values of 14.10, 14.36 and 5.13 wt.% (accounting for 75-85%), respectively. These observations could be explained as follows.

Differing from one-step pyrolysis, devolatilisation stage and secondary reaction stage could be partial or full separated by selecting distinctive intermediate feedstocks in two-step pyrolysis, and their contributions on the formation of NO_x precursors could be more easily distinguished. It was demonstrated in Section 3.3.2 that secondary reactions to produce NO_x precursors would be inhibited more significantly with the changing

intermediate feedstocks from 300 to 500 °C during their re-pyrolysis, especially for intermediate feedstock-500. Based on the formation of NO_x precursors, as for HCN-N yield, the obvious drop in two-step pyrolysis was mainly caused by its weaker secondary reactions (dehydrogenation[21] and ring-opening reactions[16]) compared with one-step pyrolysis. Meanwhile, the more dramatic drop for specific intermediate feedstock along with devolatilisation process further indicated that the formation of HCN-N for three samples was rarely linked with primary pyrolysis (sustained dehydrogenation of fuel-N)[8], while largely correlate with secondary reactions of tar-N (dehydrogenation reaction)[2, 3]. With regard to NH_3-N yield, its relevant secondary reactions (deamination, decomposition and hydrogenation reactions) in two-step pyrolysis would also become weaker from intermediate feedstock-300 to intermediate feedstock-500, inevitably leading to a gradual decrement. Most importantly, primary pyrolysis at devolatilisation stage was essential to the formation of NH_3 for three industrial biowastes due to their liable fuel-N types and subsequent nitrogen intermediates[16, 28, 29].

Subsequently, a slight decrease for PMW (2.48 wt.%) and SS (5.37 wt.%) might be explained by that NH_3-N yield was more significantly determined by primary pyrolysis in protein/amino acid/inorganic-N system, largely making up the loss caused by weaker secondary reactions. By comparison, a moderate decrease for MFW (13.62 wt.%) was probably due to that NH_3-N formation was also deeply influenced by secondary reactions besides the main contribution of primary pyrolysis in polyamide system. This phenomenon could well correspond to the results referring to change of NH_3-N yield for three samples at high temperatures (see Section 3.2.2).

In summary, it was concluded that step pyrolysis would be favorable for inhibiting the formation of NO_x precursors. During two-step pyrolysis, the intensities of reaction pathways between primary pyrolysis and secondary reaction stages could be regulatory by employing specific intermediate feedstocks for re-pyrolysis. In such case, yield of each NO_x precursor-N could be controlled with a greater impact on HCN-N than NH_3-N. Compared with one-step pyrolysis (suitable thermal utilization temperature: 800 °C), total yield of NO_x precursor-N in two-step pyrolysis could be minimized by 36-43% for three samples, indicating that step pyrolysis had its great potential and capacity in regulating the formation of NO_x precursors for N-rich industrial biowastes. These findings could provide some effective thoughts and approaches on the control of nitrogenous pollution emission during their thermal reutilization.

4. Conclusions

Step pyrolysis of three N-rich industrial biowastes was conducted to explore decisive pathways and regulatory mechanisms of NO_x precursor formation. For one-step pyrolysis of three samples, NO_x precursor-N mainly

involved considerable NH_3-N at low temperatures, which was due to primary pyrolysis of labile amide-N/inorganic-N in fuels. Meanwhile, NO_x precursor-N differed in the increment of each species yield while resembled in the total yield (20-45 wt.%) at high temperatures, which depended on specific prevailing reaction pathways linking with distinctive amide-N types. Compared with one-step pyrolysis under a same pyrolysis condition, two-step pyrolysis could minimize NO_x precursor-N yield by 36-43% with a greater impact on HCN-N (75-85%) than NH_3-N (9-37%) by manipulating intensities of reaction pathways at different stages. Subsequently, it was suggested that two-step pyrolysis was an effective way to inhibit the formation of NO_x precursors during pyrolysis of industrial biowastes, which could to some extent provide guidance on controlling N-pollution emission during their thermal reutilization.

Acknowledgments

References

[1] H.F. Chen, Y. Wang, G.W. Xu, K. Yoshikawa, Fuel-N evolution during the pyrolysis of industrial biomass wastes with high nitrogen content, Energies 5 (2012) 5418-5438.

[2] F.J. Tian, B.Q. Li, Y. Chen, C.Z. Li, Formation of NO_x precursors during the pyrolysis of coal and biomass. Part V. Pyrolysis of a sewage sludge, Fuel 81 (2002) 2203-2208.

[3] H.F. Chen, T. Namioka, K. Yoshikawa, Characteristics of tar, NO_x precursors and their absorption performance with different scrubbing solvents during the pyrolysis of sewage sludge, Appl. Energ 88 (2011) 5032-5041.

[4] J.P. Cao, L.Y. Li, K. Morishita, X.B. Xiao, X.Y. Zhao, X.Y. Wei, T. Takarada, Nitrogen transformations during fast pyrolysis of sewage sludge, Fuel 104 (2013) 1-6.

[5] L.H. Wei, L. Wen, T.H. Yang, N. Zhang, Nitrogen transformation during sewage sludge pyrolysis, Energ. Fuel 29 (2015) 5088-5094.

[6] M. Becidan, O. Skreiberg, J.E. Hustad, NO_x and N_2O precursors (NH_3 and HCN) in pyrolysis of biomass residues, Energ. Fuel 21 (2007) 1173-1180.

[7] P. Girods, A. Dufour, Y. Rogaurne, C. Rogaurne, A. Zoulalian, Pyrolysis of wood waste containing urea-formaldehyde and melamine-formaldehyde resins, J. Anal. Appl. Pyrol. 81 (2008) 113-120.

[8] H. Zhan, X.L. Yin, Y.Q. Huang, H.Y. Yuan, C.Z. Wu, NO_x precursors evolving during rapid pyrolysis of lignocellulosic industrial biomass wastes, Fuel 207 (2017) 438-448.

[9] X.D. Zhu, S.J. Yang, L. Wang, Y.C. Liu, F. Qian, W.Q. Yao, S.C. Zhang, J.M. Chen, Tracking the conversion of nitrogen during pyrolysis of antibiotic mycelial fermentation residues using XPS and TG-FTIR-MS technology, Environ. Pollut. 211 (2016) 20-27.

[10] H. Zhan, X.L. Yin, Y.Q. Huang, X.H. Zhang, H.Y. Yuan, J.J. Xie, C.Z. Wu, Characteristics of NO_x precursors and their formation mechanism during pyrolysis of herb residues, J. Fuel Chem. Technol. 45 (2017) 279-288.

[11] F. Winter, C. Wartha, H. Hofbauer, NO and N_2O formation during the combustion of wood, straw, malt waste and peat, Bioresource Technol. 70 (1999) 39-49.

[12] K.M. Hansson, J. Samuelsson, C. Tullin, L.E. Amand, Formation of HNCO, HCN, and NH_3 from the pyrolysis of bark and nitrogen-containing model compounds, Combust. Flame 137 (2004) 265-277.

[13] M. Balat, M. Balat, E. Kirtay, H. Balat, Main routes for the thermo-conversion of biomass into fuels and chemicals. Part 1: Pyrolysis systems, Energ. Convers. Manage. 50 (2009) 3147-3157.

[14] F.J. Tian, J.L. Yu, L.J. Mckenzie, J.I. Hayashi, T. Chiba, C.Z. Li, Formation of NO_x precursors during the pyrolysis of coal and biomass. Part VII. Pyrolysis and gasification of cane trash with steam, Fuel 84 (2005) 371-376.

[15] K. Tian, W.J. Liu, T.T. Qian, H. Jiang, H.Q. Yu, Investigation on the evolution of n-containing organic compounds during pyrolysis of sewage sludge, Environ. Sci. Technol. 48 (2014) 10888-10896.

[16] Y. Tian, J. Zhang, W. Zuo, L. Chen, Y.N. Cui, T. Tan, Nitrogen conversion in relation to NH_3 and HCN during microwave pyrolysis of sewage sludge, Environ. Sci. Technol. 47 (2013) 3498-3505.

[17] N.L. Panwar, R. Kothari, V.V. Tyagi, Thermo chemical conversion of biomass - Eco friendly energy routes, Renew. Sust. Energ. Rev. 16 (2012) 1801-1816.

[18] R.K. Sharma, W.G. Chan, J.I. Seeman, M.R. Hajaligol, Formation of low molecular weight heterocycles and polycyclic aromatic compounds (PACs) in the pyrolysis of α-amino acids, J. Anal. Appl. Pyrol. 66 (2003) 97-121.

[19] Y. Cao, Y. Wang, J.T. Riley, W.P. Pan, A novel biomass air gasification process for producing tar-free higher heating value fuel gas, Fuel Process. Technol. 87 (2006) 343-353.

[20] H.F. Chen, P.T. Zhao, Y. Wang, G.W. Xu, Y. Kunio, NO Emission control during the decoupling combustion of industrial biomass wastes with a high nitrogen content, Energ. Fuel 27 (2013) 3186-3193.

[21] K.M. Hansson, L.E. Amand, A. Habermann, F. Winter, Pyrolysis of poly-L-leucine under combustion-like

conditions, Fuel 82 (2003) 653-660.

[22] P. McKendry, Energy production from biomass (part 1): overview of biomass, Bioresource Technol. 83 (2002) 37-46.

[23] C. He, A. Giannis, J.Y. Wang, Conversion of sewage sludge to clean solid fuel using hydrothermal carbonization: Hydrochar fuel characteristics and combustion behavior, Appl. Energ 111 (2013) 257-266.

[24] G.Y. Zhang, D.C. Ma, C.N. Peng, X.X. Liu, G.W. Xu, Process characteristics of hydrothermal treatment of antibiotic residue for solid biofuel, Chem. Eng. J. 252 (2014) 230-238.

[25] F.X. Collard, J. Blin, A review on pyrolysis of biomass constituents: Mechanisms and composition of the products obtained from the conversion of cellulose, hemicelluloses and lignin, Renew. Sust. Energ. Rev. 38 (2014) 594-608.

[26] B. Guo, L. Gong, E. Duan, R. Liu, A. Ren, J. Han, W. Zhao, Characteristics of penicillin bacterial residue, J. Air Waste Manage. 62 (2012) 485-488.

[27] H. Liu, Q. Zhang, H.Y. Hu, P. Liu, X.W. Hu, A.J. Li, H. Yao, Catalytic role of conditioner CaO in nitrogen transformation during sewage sludge pyrolysis, P. Combust. Inst. 35 (2015) 2759-2766.

[28] J. Li, Z.Y. Wang, X. Yang, L. Hu, Y.W. Liu, C.X. Wang, Evaluate the pyrolysis pathway of glycine and glycylglycine by TG-FTIR, J. Anal. Appl. Pyrol. 80 (2007) 247-253.

[29] J. Li, Y.W. Liu, J.Y. Shi, Z.Y. Wang, L. Hu, X. Yang, C.X. Wang, The investigation of thermal decomposition pathways of phenylalanine and tyrosine by TG-FTIR, Thermochim. Acta 467 (2008) 20-29.

[30] H. Zhan, H.Y. Zhang, X.L. Yin, C.Z. Wu, Formation of nitrogenous pollutants during biomass thermo-chemical conversion, Prog. Chem. 28 (2016) 1880-1890.

[31] H. Zhan, X.L. Yin, Y.Q. Huang, H.Y. Yuan, J.J. Xie, C.Z. Wu, Z.X. Shen, J.J. Cao, Comparisons of formation characteristics of NO_x precursors during pyrolysis of lignocellulosic industrial biomass wastes, Energ. Fuel 31 (2017) 9557-9567.

[32] O. Debono, A. Villot, Nitrogen products and reaction pathway of nitrogen compounds during the pyrolysis of various organic wastes, J. Anal. Appl. Pyrol. 114 (2015) 222-234.

[33] S.S. Choi, J.E. Ko, Analysis of cyclic pyrolysis products formed from amino acid monomer, J. Chromatogr. A 1218 (2011) 8443-8455.

[34] N. Gallois, J. Tempher, S. Derenne, Pyrolysis-gas chromatography-mass spectrometry of the 20 protein amino acids in the presence of TMAH, J. Anal. Appl. Pyrol. 80 (2007) 216-230.

[35] S.S. Choi, J.E. Ko, Dimerization reactions of amino acids by pyrolysis, J. Anal. Appl. Pyrol. 89 (2010) 74-86.

[36] J.R. Pels, F. Kapteijn, J.A. Moulijn, Q. Zhu, K.M. Thomas, Evolution of nitrogen functionalities in carbonaceous materials during pyrolysis, Carbon 33 (1995) 1641-1653.

[37] C.Z. Li, L.L. Tan, Formation of NO_x and SO_x precursors during the pyrolysis of coal and biomass. Part III. Further discussion on the formation of HCN and NH_3 during pyrolysis, Fuel 79 (2000) 1899-1906.

Highlights

- Step pyrolysis of industrial biowastes was used to regulate NO_x precursor emission.

- Primary pyrolysis of labile fuel-N led to massive NH_3-N(dominant) at low temperatures.

- A varying total yield of 20-45 wt.% was observed for samples at high temperatures.

- Comparatively, two-step pyrolysis could minimize NO_x precursor-N yield by 36-43%.

- Two-step pyrolysis inhibited HCN-N(by 75-85%) more obviously than NH_3-N(by 9-37%).

[38]